

- [14] a) H. Jia, G. Zhu, B. Vugrinovich, W. Kataphinan, D. H. Reneker, P. Wang, *Biotechnol. Prog.* **2002**, *18*, 1027. b) M. M. Demir, M. A. Gulgun, Y. Z. Menceoglu, B. Erman, S. S. Abramchuk, E. E. Makhava, A. R. Khokhlov, V. G. Matveeva, M. G. Sulman, *Macromolecules* **2004**, *37*, 1787. c) E. R. Kenawy, G. L. Bowlin, K. Mansfield, J. Layman, E. Sanders, D. G. Simpson, G. E. Wnek, *Polym. Prepr. (Am. Chem. Soc., Div. Poly. Chem.)* **2002**, *43*, 457. d) K. Kim, Y. K. Luu, C. Chang, D. Fang, B. S. Hsiao, B. Chu, M. Hadjiargyrou, *J. Controlled Release* **2004**, *98*, 47. e) X. Wang, S. H. Lee, C. Drew, K. J. Senecal, J. Kumar, L. A. Samuelson, *Polym. Mater.: Sci. Eng.* **2001**, *85*, 617. f) Y. Zhang, H. Dong, I. D. Norris, A. G. MacDiarmid, W. E. J. Jones, *Polym. Mater.: Sci. Eng.* **2001**, *85*, 622. g) X. Wang, C. Drew, S. H. Lee, K. J. Senecal, J. Kumar, L. A. Samuelson, *Nano Lett.* **2002**, *2*, 1273.
- [15] a) Z. Sun, E. Zussman, A. L. Yarin, J. H. Wendorff, A. Greiner, *Adv. Mater.* **2003**, *15*, 1929. b) Y. Zhang, Z. M. Huang, X. Xu, C. T. Lim, S. Ramakrishna, *Chem. Mater.* **2004**, *16*, 3406.
- [16] D. Li, Y. Xia, *Nano Lett.* **2004**, *4*, 933.
- [17] D. Li, J. T. McCann, Y. Xia, *Small* **2005**, *1*, 83.
- [18] T. Hongu, G. O. Phillips, *New Fibres*, 2nd ed., Horwood, Cambridge, UK **1997**.
- [19] P. Gupta, G. L. Wilkes, *Polymer* **2003**, *44*, 6353.
- [20] N. Giordano, J. T. Cheng, *J. Phys.: Condens. Matter* **2001**, *13*, R271.
- [21] K. H. Lee, H. Y. Kim, Y. J. Ryu, K. W. Kim, S. W. Choi, *J. Polym. Sci., Part B: Polym. Phys.* **2003**, *41*, 1256.
- [22] M. M. Demir, I. Yilgor, E. Yilgor, B. Erman, *Polymer* **2002**, *43*, 3303.
- [23] D. H. Reneker, W. Kataphinan, A. Theron, E. Zussman, A. L. Yarin, *Polymer* **2002**, *43*, 6785.
- [24] J. K. Gimzewski, C. Gerber, E. Meyer, R. R. Schlittler, *Chem. Phys. Lett.* **1994**, *217*, 589.
- [25] P. Kim, C. M. Lieber, *Science* **1999**, *286*, 2148.

## Achieving High Density of Adsorbed Hydrogen in Microporous Metal Organic Frameworks\*\*

By Jeong Yong Lee, Long Pan, Sean P. Kelly, Jacek Jagiello, Thomas J. Emge, and Jing Li\*

In recent years, there has been an increasing demand for the development of clean and efficient energy sources/carriers to replace fossil fuels. Seeking renewable energy sources/carriers that are clean and abundant is imperative.<sup>[1,2]</sup> Hydrogen is the most abundant element in the universe and has great

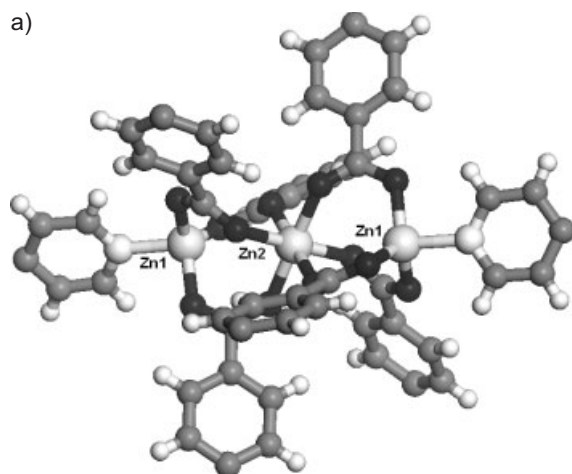
potential to become one of the dominant energy carriers in the future. Moreover, the sole by-product of the reactions between hydrogen and oxygen in the generation of energy is water, an environmentally clean species, which is another significant advantage, making this fuel superior to petroleum or other energy sources being used currently.<sup>[3]</sup> However, due to its low volumetric energy density, adequate storage of hydrogen becomes a key issue that must be addressed if the hydrogen economy is to be developed. The question is how to pack hydrogen into as small a space as possible without using excessively high pressure or very low temperature. This need has led to an intense search for efficient storage materials, but, unfortunately, no current technologies are good enough for commercialization.<sup>[4]</sup>

Recently, we have begun to explore a new type of storage media, microporous metal organic frameworks (MMOFs), a subset of the general family of metal organic frameworks (MOFs). The MMOFs contain very small pores with pore dimensions in the range of micropores ( $< 20 \text{ \AA}$ ), often ultramicropores ( $< 7 \text{ \AA}$ ). They exhibit similar sorption properties to other porous materials characteristic of physisorption, including carbon-based materials, silica, and alumina. However, they also demonstrate some apparent advantages over these systems.<sup>[5]</sup> For example, the MMOFs incorporate metals that are likely to interact with adsorbed hydrogen more strongly than other types of sorbents. They contain perfectly ordered channels that allow hydrogen to effectively access the interior space. The synthesis is simple, highly reproducible, and cost-effective. Furthermore, the crystal structures and pore properties of MMOFs can be systematically modified to improve hydrogen uptake. In this communication, we report low-temperature (77 and 87 K) hydrogen-sorption properties and a high density of adsorbed hydrogen in two MMOFs with closely related crystal structures,  $[\text{Zn}_3(\text{bpdc})_3\text{bpy}]\cdot 4\text{DMF}\cdot \text{H}_2\text{O}$  and  $[\text{Co}_3(\text{bpdc})_3\text{bpy}]\cdot 4\text{DMF}\cdot \text{H}_2\text{O}$  (bpdc = biphenyldicarboxylate; bpy = 4,4'-bipyridine; DMF = *N,N*-dimethylformamide). We illustrate how the metal centers and pore structures can affect hydrogen uptake and present isosteric heats of adsorption ( $Q_{\text{st}}$ ), calculated for the first time, for metal carboxylate-based framework structures.

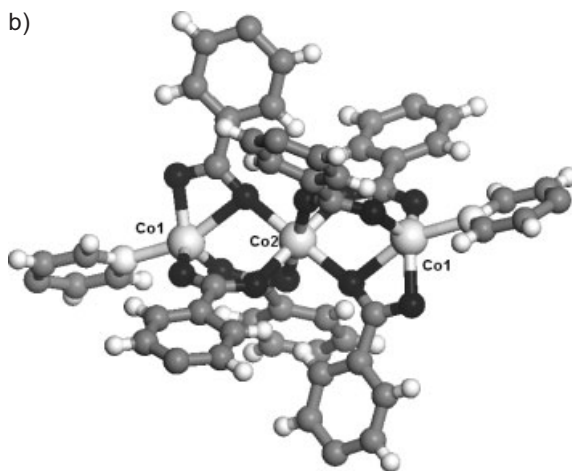
Colorless column-shaped crystals of  $[\text{Zn}_3(\text{bpdc})_3\text{bpy}]\cdot 4\text{DMF}\cdot \text{H}_2\text{O}$  (**1**) were grown in solvothermal reactions using a precursor,  $\text{Zn}(\text{bpdc})(\text{H}_2\text{O})_2\cdot \text{H}_2\text{O}$ .<sup>[6]</sup> Compound **1** was insoluble in common organic solvents, but could be converted to the precursor upon refluxing with mixed solvents of  $\text{H}_2\text{O}/\text{EtOH}$  (1:10). Crystals of **1** can also be grown by reactions of  $\text{Zn}(\text{NO}_3)_2\cdot 6\text{H}_2\text{O}$ , bpdc, and bpy in DMF (molar ratio of 1:1:0.65). Single-crystal X-ray diffraction showed that the crystal structure of **1** is different but closely related to  $[\text{Co}_3(\text{bpdc})_3\text{bpy}]\cdot 4\text{DMF}\cdot \text{H}_2\text{O}$  (**2**).<sup>[7]</sup> The structure of **1** possesses two crystallographically independent zinc centers (Zn1 and Zn2).<sup>[8]</sup> Two Zn1 atoms and a Zn2 atom form a trinuclear metal cluster  $[\text{Zn}_3(\text{bpdc})_6(\text{bpy})_2]$ . As shown in Figure 1a, this building block is composed of one octahedral metal (Zn2) located at the center and two tetrahedral metals (Zn1) situated at two ends.

[\*] Prof. J. Li, J. Y. Lee, Dr. L. Pan, S. P. Kelly, Dr. T. J. Emge  
Department of Chemistry and Chemical Biology, Rutgers University  
610 Taylor Road, Piscataway, NJ 08854 (USA)  
E-mail: jingli@rutchem.rutgers.edu  
Dr. J. Jagiello  
Quantachrome Instruments  
1900 Corporate Drive, Boynton Beach, FL 33426 (USA)

[\*\*] We are grateful to the financial support from the National Science Foundation (DMR-0422932). Acknowledgment is also made to the donors of The Petroleum Research Fund, administered by the ACS, for the partial support of this research. Supporting Information is available online from Wiley InterScience or from the author.



1



2

**Figure 1.** a) The  $\text{Zn}_3$  unit of **1**. The two terminal (outer) Zn atoms (Zn1) have a tetrahedral coordination and the center Zn atom (Zn2) has an octahedral coordination. b) The  $\text{Co}_3$  unit of **2**. The two outer Co atoms (Co1) have a trigonal bipyramidal coordination, and the center Co atom (Co2) has an octahedral coordination. Zn and Co (light gray, large balls), O (black balls), N (light gray, medium-sized balls), C (gray), and H (light gray, small balls).

The metal nodes are connected to adjacent nodes by carboxylate groups from six bpdc ligands located in the equatorial plane to form two-dimensional (2D) double layers; the remaining two apical positions of the Zn1 are bound to nitrogen atoms of bpy to give rise to a three-dimensional (3D) pillared framework. Two such identical networks interpenetrate to generate 1D channels as shown in Figure 2a.

These 1D channels possess a unique internal surface structure, in that they are composed of alternating large-diameter cages ( $\sim 10.6 \text{ \AA} \times 10.6 \text{ \AA} \times 5 \text{ \AA}$ , calculated based on van der Waals' radius of carbon) and smaller windows (triangular in shape with an effective maximum dimension of  $\sim 8 \text{ \AA}$ ). They are similar but

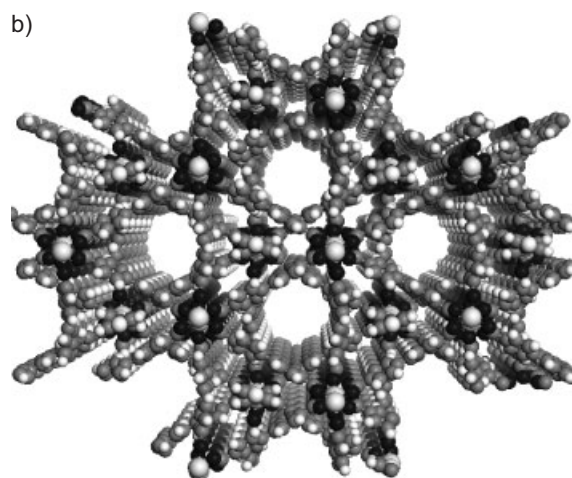
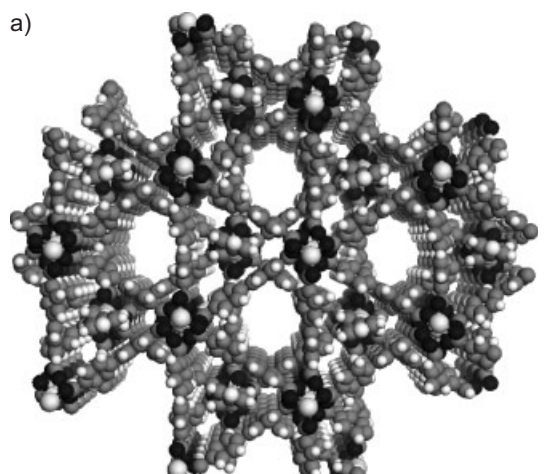


**Figure 2.** a) View of structure **1** showing 1D channels. b) View of structure **2** showing the similar channels. The same grayscale scheme as in Figure 1 is used here.

not identical to those in **2** (Fig. 2b).<sup>[7]</sup> The channels are filled with four DMF molecules and a water molecule.

The most obvious difference between the two structures **1** and **2** is in the coordination number of the outer metals of the  $\text{M}_3$  unit, which is 4 for **1** and 5 for **2**, although the fifth metal coordination bond of **2** has a Co–O bond length of  $2.32 \text{ \AA}$ , which is rather long, but the equivalent fifth Zn–O bond,  $2.8 \text{ \AA}$  in length, is too long to be considered a bond. The other three metal–oxygen bonds of the outer metals are in the ranges  $1.94\text{--}1.95 \text{ \AA}$  for **1** and  $1.94\text{--}2.01 \text{ \AA}$  for **2**. However, this difference in coordination number does not cause any striking difference in the overall motif and topology of the structure, because the same twists and rotations of the bpdc ligands in **1** are achieved in **2**, but without the fifth Zn–O bond on each outer metal. Thus, the crystal packing motif is nearly the same (i.e., nearly isomorphous) in **1** and **2**. On the other hand, based upon the unit-cell packing diagram with the solvent molecules omitted (Fig. 2), **1** appears to have the six-membered rings rotated somewhat more into the chan-

nel than **2** does, so that the channels in **1** have more surface atoms sticking in the voids. These rotational differences of ligands for **1** versus **2** are also evident in the side-by-side diagrams of the (closest-ring) coordination spheres of **1** and **2** shown in Figure 1. Examination of key torsion angles for adjacent six-membered rings and metal atoms quantifies this difference. Also indicative of conformational differences that lead to a different accessible volume<sup>[9]</sup> in **1** and **2** are the dihedral angles between six-membered rings whose centers-of-mass are inversion related (through the central metal atom) in the respective coordination spheres of **1** and **2**.

To experimentally evaluate the pore characteristics of the two structures and to analyze their hydrogen-adsorption properties, as well as to understand the differences in their pore structures, we carried out an extensive gas-adsorption study at cryogenic temperatures (77 and 87 K). We repeatedly measured argon adsorption–desorption isotherms at 87 K and hydrogen adsorption–desorption isotherms at both 77 and 87 K at pressures below and up to 1 atm (1 atm ~ 101.3 kPa). Ar was selected for the characterization of pore properties of both **1** and **2**, mainly for the following reasons: First, Ar has a smaller kinetic diameter than N<sub>2</sub>, and thus, Ar can penetrate smaller pores.<sup>[10]</sup> Second, interactions of Ar with solids are non-specific, while the N<sub>2</sub> molecule has a permanent quadrupole moment and thus interacts specifically with the external electric field of the solid. These interactions increase the effective adsorption energy of N<sub>2</sub> and shift the adsorption isotherms of N<sub>2</sub> to lower relative pressures compared to Ar. Specific interactions of N<sub>2</sub> also contribute to its lower diffusion rates into micropores, and such an effect becomes significant for structures that have very small pore diameters. We performed powder X-ray diffraction (PXRD) analysis on all samples before and after the adsorption measurements to ensure their purity and structure integrity. The results obtained were highly reproducible and represent a well-defined measure of the hydrogen- and argon-adsorption capacity. The argon sorption follows a typical type I isotherm with an estimated Brunauer–Emmett–Teller (BET) surface area of 792 and 922 m<sup>2</sup>g<sup>−1</sup> for **1** and **2**, respectively. The hydrogen adsorption–desorption isotherms for **1** and **2** at 77 and 87 K are plotted in Figure 3.

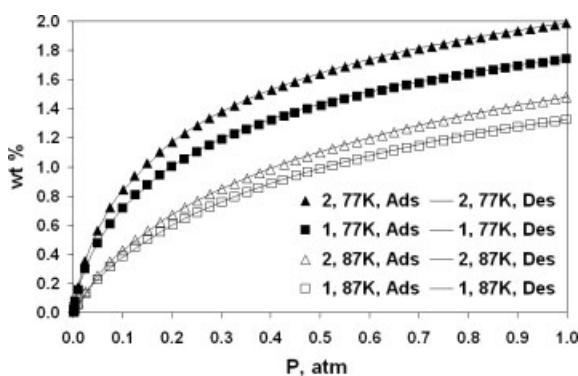


**Figure 3.** H<sub>2</sub> adsorption (Ads) and desorption (Des) isotherms at 77 and 87 K for **1** and **2**, respectively.

No hysteresis was observed in these isotherms. It is interesting to see the difference in the hydrogen uptake in the two structures. The Co structure (**2**) adsorbs more hydrogen than the Zn structure (**1**) at both temperatures and all pressure levels. At 87 K and 1 atm, the values are 1.32 and 1.48 wt.-% for **1** and **2**, respectively. At 77 K, they are 1.74 and 1.98 wt.-% for **1** and **2**, respectively. This difference is in agreement with the estimated total micropore volume obtained from Ar adsorption data at 87 K, which are 0.33 and 0.38 cm<sup>3</sup>g<sup>−1</sup> for **1** and **2**, respectively. Note that the hydrogen uptakes at these temperatures correspond to the highest gravimetric densities among porous metal organic structures reported thus far (0.9–2.0 wt.-%).<sup>[11–14]</sup> The amount of hydrogen adsorbed in both **1** and **2** is significantly higher than that absorbed in ZSM-5 (0.7 wt.-%)<sup>[15]</sup> and H-SSZ-13 (1.28 wt.-%).<sup>[16]</sup> The latter was recently reported to have the highest uptake value of hydrogen among zeolite materials. It is also worth noting that the densities of the adsorbed H<sub>2</sub> at 77 K and 1 atm are 0.052–0.053 g cm<sup>−3</sup> in **1** and **2**, calculated based on the estimated pore volumes using Ar sorption data at 87 K. These values represent the highest densities of H<sub>2</sub> in any porous metal organic framework structures reported thus far.<sup>[11–14]</sup> and are comparable to those of liquid H<sub>2</sub> (e.g., 0.053 g cm<sup>−3</sup> at 30 K and 8.1 atm, or 0.03 g cm<sup>−3</sup> at critical point 33 K and 13 atm).<sup>[17]</sup>

The isosteric heat of adsorption ( $Q_{st}$ ) is a differential quantity based on the Clausius–Clapeyron equation.<sup>[18]</sup> It is related to the energy of H<sub>2</sub> adsorption and can be considered a measure of the extent of sorbent–sorbate interactions in a porous material. The  $Q_{st}$  values can be calculated using hydrogen-adsorption isotherms measured at different temperatures. We have performed a calculation of the isosteric heats of hydrogen adsorption in both **1** and **2** using 77 and 87 K isotherms. The calculated  $Q_{st}$  data represent the first set for metal carboxylate framework structures and they are plotted in Figure 4 with estimated error bars. The  $Q_{st}$  values are higher for **2** than for **1** over the weight range 0.1–1.3 %, indicative of somewhat stronger sorbent–sorbate interactions, and, thus, higher energy of hydrogen adsorption, in **2**. The  $Q_{st}$  values of both **1** and **2** decrease as the hydrogen uptake increases.

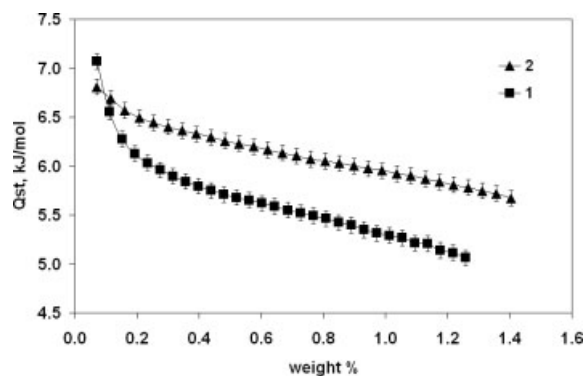


**Figure 4.** Isosteric heats of H<sub>2</sub> adsorption for **1** (■) and **2** (▲) as functions of the amount of hydrogen adsorbed. Estimated error bars for the  $Q_{st}$  values are also indicated in the figure.

In summary, an investigation of the hydrogen-adsorption properties of the two MOFs  $[M_3(\text{bpdc})_3\text{bpy}]\cdot 4\text{DMF}\cdot \text{H}_2\text{O}$  [ $M = \text{Zn}(\mathbf{1})$ ,  $\text{Co}(\mathbf{2})$ ] at low temperatures has revealed very interesting adsorption properties. The hydrogen uptakes (wt.-%) at 77 K (or 87 K) and 1 atm are 1.74 (1.32) and 1.98 (1.48) for **1** and **2**, respectively, among the highest values reported so far for metal-organic-based porous materials. The study also suggests that the difference in the  $\text{H}_2$  uptake between the two structures can be attributed to their pore volumes (0.33 and  $0.38 \text{ cm}^3 \text{ g}^{-1}$  for **1** and **2**, respectively), as well as the extent of gas–solid interactions, which is indicated by the isosteric heats of adsorption, calculated for the first time here for carboxylate-based metal organic structures. The high density of adsorbed  $\text{H}_2$  falls in the range of liquid  $\text{H}_2$  and suggests relatively strong sorbent–sorbate interactions in these materials with very small pores.

## Experimental

$[\text{Zn}_3(\text{bpdc})_3\text{bpy}]\cdot 4\text{DMF}\cdot \text{H}_2\text{O}$  (**1**) was prepared by mixing 0.08 g of  $[\text{Zn}(\text{bpdc})(\text{H}_2\text{O})_2]\cdot \text{H}_2\text{O}$  (white powder) and 0.125 g of bpy in 5 mL of DMF. The mixture was transferred to an acid-digestion bomb, sealed, and heated at  $150^\circ\text{C}$  for 3 days. After washing with  $3 \times 10 \text{ mL}$  of DMF and drying in air, colorless columnar crystals of **1** were isolated in high yield (94 %). 10 mg of the ground product of **1** was added to a solution of water and ethanol (in 1:10 ratio) and refluxed for 30 min to yield 1D  $[\text{Zn}(\text{bpdc})(\text{H}_2\text{O})_2]\cdot \text{H}_2\text{O}$  in high yield (>90 %). Crystal samples of **1** used in sorption experiments were grown by reactions of  $\text{Zn}(\text{NO}_3)_2\cdot 6\text{H}_2\text{O}$  (0.059 g) with bpdc (0.048 g) and bpy (0.031 g) in 10 mL of DMF in the molar ratio 1:1:0.65 at  $150^\circ\text{C}$  for 48 h. Reactants were mixed in a Teflon-lined autoclave and heated in an oven at a constant temperature. After the reaction, the autoclave was allowed to cool to room temperature. The solution was filtered, the product was washed with DMF ( $3 \times 10 \text{ mL}$ ), and the crystals were dried at  $80^\circ\text{C}$  for 3 h. The purple-colored column-shaped crystals of **2** were grown by mixing  $\text{Co}(\text{NO}_3)_2\cdot 6\text{H}_2\text{O}$  (0.020 g) with bpdc (0.025 g) and bpy (0.016 g) in DMF (5 mL) in the molar ratio 1:1.45:1.45:0.94, followed by heating at  $150^\circ\text{C}$  for 48 h. The same filtering and drying conditions of **1** were applied to **2**. Single-crystal X-ray diffraction data were collected on a Bruker CCD (charge-coupled device) system with graphite monochromated Mo K $\alpha$  radiation [19].

Hydrogen isotherms were measured in the pressure range 0.001–1.0 atm using an Autosorb 1 MP (Quantachrome Instruments, Boynton Beach, FL). Experimental temperatures of 77.3 and  $87.5 \text{ K}$  were maintained using liquid nitrogen and a liquid argon bath, respectively. Prior to the adsorption measurements, both samples **1** and **2** were degassed at 373 K and under high vacuum for 6–8 h.

Received: April 26, 2005

Final version: June 29, 2005

Published online: September 29, 2005

- [7] L. Pan, H.-M. Liu, X.-G. Lei, X.-Y. Huang, D. H. Olson, N. J. Turro, J. Li, *Angew. Chem. Int. Ed.* **2003**, 42, 542.  $[\text{M}_3(\text{bpdc})_3\text{bpy}]\cdot 4\text{DMF}\cdot \text{H}_2\text{O}$  ( $M = \text{transition and post transition metal}$ ) also belong to the Rutgers RPM (Recyclable Porous Materials) series.
- [8] Crystal data for **1** ( $\text{C}_{64}\text{H}_{61.4}\text{N}_{6.7}\text{O}_{16.7}\text{Zn}_3$ ): molecular weight  $M_w = 1377.88$ , monoclinic,  $P2_1/n$  (no. 14),  $a = 14.608(3)$ ,  $b = 18.041(4)$ ,  $c = 24.803(5) \text{ \AA}$ ,  $\beta = 90.005(1)$ ,  $V = 6537(2) \text{ \AA}^3$ ,  $Z = 4$ ,  $T = 100 \text{ K}$ ,  $\rho_{\text{calcd}} = 1.400 \text{ g cm}^{-3}$ , Mo K $\alpha$  radiation,  $\mu = 18.74 \text{ cm}^{-1}$ , colorless block  $0.12 \text{ mm} \times 0.08 \text{ mm} \times 0.05 \text{ mm}$ ; 58950 measured reflections,  $F^2$  refinement,  $R_1 = 0.044$ ,  $wR_2 = 0.104$ , 11515 independent observed absorption-corrected reflections [ $I > 2\sigma(I)$ ],  $2\theta = 52.75^\circ$ , 836 parameters; 57:43 twinning matrix (10001000-1). For desolvated crystals,  $\rho = 1.090 \text{ g cm}^{-3}$  (100 K) and  $1.067 \text{ g cm}^{-3}$  (293 K) for **1** and **2**, respectively. CCDC 240928 contains the supplementary crystallographic data for this paper. These data can be obtained free of charge from The Cambridge Crystallographic Data Centre via [www.ccdc.cam.ac.uk/data\\_request/cif](http://www.ccdc.cam.ac.uk/data_request/cif).
- [9] Using the SOLV routine in PLATON, volumes of potential solvent area (SA) were found to be  $2658 \text{ \AA}^3$  (40.7 %) and  $2812 \text{ \AA}^3$  (42.4 %) for **1** and **2**, respectively. SA is sometimes termed “accessible volume”. a) A. L. Spek, *Acta Crystallogr., Sect. A: Found. Crystallogr.* **1990**, A46, C-34. A. L. Spek, *J. Appl. Crystallogr.* **2003**, 36, 7. b) A. L. Spek, *PLATON, A Multipurpose Crystallographic Tool*, Utrecht University, Utrecht, The Netherlands **2005**.
- [10] D. W. Breck, *Zeolite Molecular Sieves*, Wiley, New York **1974**.
- [11] a) D. N. Dybtsev, H. Chun, S. H. Yoon, D. Kim, K. Kim, *J. Am. Chem. Soc.* **2004**, 126, 32. b) D. N. Dybtsev, H. Chun, K. Kim, *Angew. Chem. Int. Ed.* **2004**, 43, 5033.
- [12] a) N. L. Rosi, J. Eckert, M. Eddaoudi, D. T. Vodak, J. Kim, M. O’Keeffe, O. M. Yaghi, *Science* **2003**, 300, 1127. b) J. C. Rowsell, A. R. Millward, K. S. Park, O. M. Yaghi, *J. Am. Chem. Soc.* **2004**, 126, 5666.
- [13] a) E. Y. Lee, M. P. Suh, *Angew. Chem. Int. Ed.* **2004**, 43, 2798. b) E. Y. Lee, S. Y. Jang, M. P. Suh, *J. Am. Chem. Soc.* **2005**, 127, 6374.
- [14] S. S. Kaye, J. R. Long, *J. Am. Chem. Soc.* **2005**, 127, 6506.
- [15] a) M. G. Nijkamp, J. E. M. J. Raaymakers, A. J. van Dillen, K. P. de Jong, *Appl. Phys. A* **2001**, 72, 619. b) J. Weitkamp, M. Fritz, S. Ernst, *Int. J. Hydrogen Energy* **1995**, 20, 967.
- [16] A. Zecchina, S. Bordiga, J. G. Vitillo, G. Ricchiardi, C. Lamberti, G. Spoto, M. Bjørger, K. P. Lillerrud, *J. Am. Chem. Soc.* **2005**, 127, 6361.
- [17] National Institute of Standards and Technology homepage. <http://www.nist.gov/> (accessed February 2005).
- [18] A. Clark, *Theory of Adsorption and Catalysis*, Academic, New York **1970**.
- [19] Bruker (2003). SAINT+ (Version 6.45), SMART (Version 5.629) and SHELXTL (Version 6.14). Bruker AXS Inc., Madison, Wisconsin, USA.

- [1] T. M. L. Wigley, R. Richels, J. A. Edmonds, *Nature* **1996**, 379, 240.
- [2] W. C. Sailor, D. Bodansky, C. Braun, S. Fetter, B. van der Zwaan, *Science* **2000**, 288, 1177.
- [3] J. A. Turner, *Science* **1999**, 285, 687.
- [4] US Department of Energy, Energy Information Portal. <http://www.eere.energy.gov/> (accessed October 2003).
- [5] L. Pan, M. Sander, X.-Y. Huang, J. Li, M. Smith, E. Bittner, B. Bockrath, J. K. Johnson, *J. Am. Chem. Soc.* **2004**, 126, 1308.
- [6] L. Pan, N. Ching, X.-Y. Huang, J. Li, *Inorg. Chem.* **2000**, 39, 5333.